CHAPTER III
PREPARATION, CHARACTERIZATION AND ANTI-BACTERIAL PROPERTIES OF ELECTROSPUN POLYACRYLONITRILE FIBROUS MEMBRANES CONTAINING SILVER NANOPARTICLES

3.1 Abstract

Fibrous membranes with antibacterial activity were prepared from 10% w/v polyacrylonitrile (PAN) solutions containing silver nitrate ($AgNO_3$) in the amounts of 0.5-2.5% by weight of PAN by electrospinning. *N,N*-Dimethylformamide (DMF) was used as both the solvent for PAN and reducing agent for Ag^+ ions. The enhancement in the reduction process was achieved with UV irradiation, which resulted in the formation of larger AgNPs in areas adjacent to and at the surface of the fibers. Without the UV treatment, the size of the AgNPs was smaller than 5 nm on average. Under the 10 min of UV treatment, the size of the particles increased with an increase in the initial $AgNO_3$ concentration in the solutions to range between 5.3-7.8 nm on average. Without or with the UV treatment, the diameters of the obtained PAN/AgNPs composite fibers decreased with an increase in the initial $AgNO_3$ concentration in the solutions, with the diameters of the obtained composite fibers that had been subjected to UV irradiation exhibiting lower values (i.e., 185-205 nm versus 194-236 nm on average). Both the cumulative amounts of the released silver and the bactericidal activities of the PAN/AgNPs composite fibrous materials against two commonly-studied bacteria, i.e., Gram-positive *Staphylococcus aureus* and Gram-negative *Escherichia coli*, increased with increases in both the initial $AgNO_3$ concentration in the solutions and the UV irradiation time interval.

(Keywords: Polyacrylonitrile, Ag nanoparticles, UV irradiation, Antibacterial activity)

3.2 Introduction

Over the past few years, there have been considerable and renewed interests on the use of silver nanoparticles (AgNPs) as a broad-spectrum antibacterial agent, due to their effectiveness and low toxicity.[1-5] Their mode of action can be one or more of the following processes: (1) Ag^+ ions inhibit adenosine triphosphate (ATP) synthesis by binding to an ATP synthase, (2) Ag^+ ions enter the cell and bind with DNA, leading to denaturation of DNA and (3) Ag^+ ions block the respiratory chain of microorganisms in the cytochrome c oxidase and succinate-semialdehyde dehydrogenase components of the cells.[6,7] Size, stability and the amount of AgNPs play major roles in determining their activity. A number of methods have been used to generate AgNPs from Ag^+ ions. Some of these are chemical reduction by sodium borohydride ($NaBH_4$),[8-10] hydrazinium hydroxide[11,12] or dimethyl formamide (DMF);[13-18] photoreduction by ultraviolet (UV) or gamma (γ) irradiation;[19-22] and simple heat treatment.[23] In most cases, the generated Ag^0 nuclei are prevented from further growth and agglomeration by a polymeric stabilizer.[24,25]

In the past two decades, electrostatic spinning or electrospinning, a well-established process capable of fabricating fibers with diameters in the range of tens of nanometers to less than ten micrometers from materials of diverse origins, has received substantial interests, owing predominantly to the ease of set-up and effectiveness in fiber formation.[26] The morphology and size of the electrospun fibers depend on a number of factors, such as solution properties (e.g., shear viscosity, electrical conductivity, surface tension, evaporation rate of the solvent, etc.), processing conditions (e.g., electrical potential, collection distance, etc.), and ambient conditions (e.g., temperature, humidity, etc.).[27-29] Due to their unique characteristics, such as high surface area to volume or mass ratio, high porosity of the obtained fiber matrices, etc., the electrospun fibers are potentially useful as scaffolding substrates for biomedical engineering, catalyst supports, sensors and filters.[29-33]

Polyacrylonitrile (PAN) is an important engineering polymer that has commonly been used to produce various types of synthetic fibers. Due to its unique thermal properties (i.e., melting point = 317 °C and glass transition temperature = 85

°C) and good solvent resistance, PAN is an ideal material for fabrication into fibers usually by a wet-spinning process or fibrous or solid film membranes for a variety of applications.[34,35] It can also be fabricated into fibers by electrospinning.[36-38] Detailed studies on the effects of some solution (e.g., solution concentration, viscosity, conductivity and surface tension) and process (e.g., applied electrostatic field strength, emitting electrode polarity, nozzle diameter, and take-up speed of a rotating-drum collector) parameters on morphology and diameters of the electrospun PAN fibers were reported by Baumgarten[36] and Sutasinpromprae et al.[37] While DMF has been used as solvent for preparing PAN solutions for electrospinning,[36,37] it is an effective reducing agent for Ag^+ ions,[13-18] with PAN molecules preventing the agglomeration of the as-formed AgNPs and facilitating the fiber formation.[38] The electrospun composite fibers containing AgNPs have also been fabricated with other polymers, e.g., cellulose acetate,[19] poly(vinyl alcohol),[20] poly(L-lactide),[39] poly(ε-caprolactone)-based polyurethane[40] and gelatin.[41]

In the present contribution, we report the preparation of PAN fibrous membranes containing AgNPs by electrospinning. Due to its high thermal and good solvent resistance properties, PAN was chosen as the matrix. The Ag^+ ions were reduced into AgNPs in two steps by means of a reducing agent, i.e., DMF, and by UV irradiation. The formation of the AgNPs was verified either qualitatively or quantitatively by UV-visible spectrophotometry, transmission electron microscopy, energy dispersive X-ray spectroscopy, and atomic absorption spectroscopy. The integrity of the AgNPs-loaded PAN fiber mats upon submersion in distilled water and under tensile loading was also studied. The release characteristic of the as-loaded silver from the membranes and the antibacterial activity of them against two commonly-studied pathogens, Gram-positive *Staphylococcus aureus* and Gram-negative *Escherichia coli*, were carefully investigated.

3.3 Experimental

3.3.1 Materials

Commercially available PAN-based fibers (Thai Acrylic Fibre Co., Ltd., Thailand) were used as the raw material for the preparation of PAN solutions. According to the information provided by the manufacturer of the PAN-base fibers, the polymer (hereafter, PAN) contains about 91.4 wt.% acrylonitrile monomer (CH_2=CHCN) and about 8.6 wt.% methyl acrylate comonomer (CH_2=CHCOOHCH$_3$), with the weight average molecular weight being about 55,500 kDa. Silver nitrate ($AgNO_3$; 99.998% purity) was purchased from Fisher Scientific (USA). *N,N*-Dimethylformamide (DMF) was purchased from Labscan Asia (Thailand). All chemicals were of analytical reagent grade and used without further purification.

3.3.2 Preparation and characterization of PAN solutions containing AgNPs

DMF was used to dissolve the PAN-based fibers to obtain the base PAN solution at the concentration of 10% w/v. Various amounts of $AgNO_3$ (i.e., 0.5, 1.5 and 2.5% by weight of PAN) were then added into the base solution. To investigate the effect of aging time on the formation of AgNPs, the $AgNO_3$-containing PAN solutions were aged in amber glass bottles under a continuous stirring for varying aging time intervals. Some of the aged $AgNO_3$-containing PAN solutions were characterized for shear viscosity and electrical conductivity using a Brookfield DV-III programmable rheometer and a SUNTEX SC-170 conductivity meter. The existence of the AgNPs that were formed within the aged $AgNO_3$-containing PAN solutions was confirmed by monitoring the surface plasmon absorption band using a Shimadzu UV-2550 UV-visible spectrophotometer.

3.3.3 Electrospinning and UV treatment

The base PAN solution and the $AgNO_3$-containing PAN solutions that had been aged for 5 d were fabricated into fiber mats by electrospinning. Firstly, each of the as-prepared solutions was loaded into a standard 10-mL glass syringe, the open end of which was attached to a blunt 20-gauge stainless steel hypodermic needle (OD = 0.91 mm), used as the nozzle. Both the syringe and the needle were tilted about 45° from a horizontal baseline. A piece of aluminum (Al) sheet wrapped around a rotating cylinder (OD and width $\approx$ 15 cm; rotational speed $\approx$ 40-50 rpm) was used as the collecting device. A Gamma High-Voltage Research ES30P-5W dc

power supply (USA) was used to charge the solution by attaching the positive emitting electrode to the nozzle and the grounding one to the collecting device. An electrical potential of 15 kV was applied across a distance of 20 cm between the tip of the needle and the outer surface of the collecting device (i.e., collection distance, measured at a right angle to the surface of the collecting device). The electrospun fiber mats were collected over a period of 48 h.

To observe the effect of UV treatment on the morphology and/or size of the electrospun fibers and the as-formed AgNPs, sets of AgNPs-loaded PAN fiber mat specimens were irradiated with UV light (λ_{max} = 254 nm; FUNA®-UV-LINKER FS-800, Japan) for either 1 or 10 min (on each side of the specimens), unless noted otherwise.

3.3.4 Physical, physico-chemical and mechanical characterization

The neat and the AgNPs-loaded PAN fiber mats were examined either qualitatively or quantitatively for the morphology and size of the individual fiber segments and/or the as-formed AgNPs by a JEOL JSM-6400 scanning electron microscope (SEM), a JEOL JEM-2100 transmission electron microscope (TEM) and an Oxford 2000 energy dispersive X-ray (EDX) facility of a Phillips PW 2400 X-ray fluorescence spectroscope. Diameters of the individual fiber segments were determined from SEM images, while those of the AgNPs were determined from TEM images, using an image-analytical software.

In the physico-chemical analysis, circular disc specimens of about 1.5 cm in diameter from both the neat and the AgNPs-loaded PAN fiber mat samples were weighed and then submerged in distilled water (pH 6.93) at room temperature for 7 d. This experimental condition was chosen based on the potential usefulness of the fiber mats as filtration membranes. The weight loss and water retention of each specimen were determined according to the following equations:

$$\text{Weight loss (\%)} = \frac{W_{di} - W_{dt}}{W_{di}} \times 100, \quad (1)$$

and

$$\text{Water retention (\%)} = \frac{W_{st} - W_{dt}}{W_{dt}} \times 100, \quad (2)$$

where W_{di} denotes the initial dry weight of each specimen and W_{dt} and W_{st} denote the

weights of the specimen in its dry and wet state, respectively, after submersion in distilled water for 7 d.

Mechanical properties of the obtained fiber mats were assessed by a Lloyd LRX universal testing machine at room temperature (i.e., 25 ± 1 °C), using a load cell of 500 N and a cross-head speed of 20 $mm \cdot min^{-1}$. All fiber mat specimens were cut into a rectangular shape with the dimensions of 70 mm × 10 mm. The gauge length was 50 mm. The thicknesses of the specimens were measured with a Mitutoyo digital micrometer.

3.3.5 Release characteristic of AgNPs-loaded PAN fiber mats

Prior to the release assay, the actual amounts of silver (either in the form of AgNPs or the residual Ag^+ ions) in the AgNPs-loaded PAN fiber mat specimens (circular disc; 2.8 cm in diameter) both before and after the UV treatment were determined. First, each specimen was dissolved in 5 mL of 95% nitric acid (HNO_3), followed by the addition of distilled water to attain the final volume of 50 mL. After that, the silver-containing solution (50 mL) was quantified for the amount of silver by means of a Varian SpectrAA-300 atomic absorption spectroscope (AAS). The release characteristics of silver (either in the form of AgNPs or the residual Ag^+ ions) from the AgNPs-loaded PAN fiber mat specimens (circular disc; 2.8 cm in diameter) both before and after the UV treatment were assessed in distilled water. Each specimen was first immersed in 50 mL of distilled water at room temperature (i.e., 25 ± 1 °C). At a specified immersion time point ranging between 0 and 7 d, 50 mL of the releasing medium was quantified for the amount of the released silver, using AAS. The obtained data were carefully calculated to obtain the cumulative amounts of the released silver. The cumulative release profiles of silver were expressed based on the unit weight of the specimens.

3.3.6 Antibacterial evaluation

Antibacterial activity of the AgNPs-loaded PAN fiber mats both before and after the UV treatment was evaluated against two commonly-studied strains of aerobic bacteria, e.g., Gram-positive *Staphylococcus aureus* (ATCC 25023) and Gram-negative *Escherichia coli* (ATCC 25922). The assessment was conducted based on the disc diffusion method of the US Clinical and Laboratory

Standards Institute (CLSI). Vancomycin and gentamicin were used as the control antibacterial drugs for *S. aureus* and *E. coli*, respectively. Each specimen (circular disc; 15 mm in diameter) and the respective control drug were placed on Difco™ Mueller Hinton agar in a Petri dish and then incubated at 37 °C for 24 h. If inhibitory concentrations were reached, there would be no growth of the microbes, which could be seen as clear or inhibition zones around the disc specimens. These were photographed for further evaluation.

3.3.7 Statistical analysis

All the data were expressed as means ± the standard errors of the means. Statistical analysis was performed based on the ANOVA, followed by Fisher's PLSD, and the significance was accepted at $p < 0.05$.

3.4 Results and Discussion

3.4.1 Formation of AgNPs in $AgNO_3$-containing PAN solutions

The reduction of Ag^+ ions into elemental Ag^0 in the form of nanoparticles (hereafter, AgNPs) takes place through a series of steps: primary nucleation, secondary nucleation or crystal growth via diffusion mechanism to obtain primary particles, and agglomeration of some adjacent primary particles into aggregated clusters (i.e., secondary particles).[42] The initial reduction of Ag^+ ions could occur via the oxidation reaction with DMF at room temperature, according to the following mechanism:

$$HCONMe_2 + 2Ag^+ + H_2O \longrightarrow 2Ag^0 + Me_2NCOOH + 2H^+. \quad (3)$$

As the reaction continued, the $AgNO_3$-containing PAN solutions changed their color from light yellow to brown, which was taken as an obvious physical evidence for the formation of AgNPs within the solutions. The formation of AgNPs within a $AgNO_3$-containing solution could be assessed from the presence of the surface plasmon band at around 420-430 nm in the UV absorption spectrum.[41] Figure 1 illustrates the UV absorption spectra of the $AgNO_3$-containing PAN solutions after having been aged for various time intervals. Though not shown, no absorption of any kind was observed for the base PAN solution.

The influence of aging time and initial concentration of $AgNO_3$ on UV absorption spectra of the $AgNO_3$-containing PAN solutions can be construed from the results shown in Figure 1. Noticeable changes in the UV absorption spectra were first observed for the solutions that had been aged for at least 1 d. Regardless of the initial $AgNO_3$ concentration, an increase in the aging time resulted in a monotonous increase in the intensity of the surface plasmon band centering around 420-430 nm, which reached a maximum value at about 6 d of aging. The change in the position of the bands as resulting from the variation in the aging time was, however, insignificant. With regard to the effect of the initial $AgNO_3$ concentration, it is expected that the intensity of the surface plasmon band at a given aging time point should increase with an increase in the $AgNO_3$ concentration. However, only the $AgNO_3$-containing PAN solutions that had been aged for at least 3 d showed a noticeable increase in the UV absorption intensity with an increase in the initial $AgNO_3$ concentration.

It has been shown that an increase in the intensity of the surface plasmon band correlates well with an increase in the number of the as-formed AgNPs, while a shift in the position of the band in the direction of a greater wavelength relates to an increase in the size of the as-formed particles.[19,41] The results shown in Figure 1 indicate clearly that DMF is an effective reducing agent for Ag^+ ions and the number of the as-formed AgNPs increased with an increase in both the time interval used to age the solutions and the initial concentration of $AgNO_3$ contained in the solutions, without having a strong influence on the size of the as-formed particles. Possible interactions between the AgNPs and the cyano-nitrogen of PAN molecules and/or the amino-nitrogen of DMF are, to some extent, effective enough to prevent the agglomeration of the as-formed particles and, at the same time, are responsible for the rather well distribution of the as-formed particles within the solutions.

Prior to electrospinning, the base PAN solution and the $AgNO_3$-containing PAN solutions that had been aged for 5 d were measured for their shear viscosity and electrical conductivity. The results are summarized in Table 1. While the addition and increasing initial concentration of $AgNO_3$ resulted in a slight increase in the shear viscosity of the solutions (i.e., from 337 mPa·s for the base

PAN solution to 363 mPa·s for the 5 d-aged 2.5% $AgNO_3$-containing PAN solution), marked increase in the electrical conductivity was clearly observed (i.e., from 58 $\mu S \cdot cm^{-1}$ for the base PAN solution to 319 $\mu S \cdot cm^{-1}$ for the 5 d-aged 2.5% $AgNO_3$-containing PAN solution). The slight increase in the shear viscosity should be a result of the presence of the as-formed AgNPs that interferes with the movement of the PAN molecules, while the marked increase in the electrical conductivity must be due to the presence of the residual Ag^+ ions, the H^+ ions as the by-product of the reduction reaction of Ag^+ ions by DMF, and the NO_3^- ions.

3.4.2 Electrospinning and effect of UV treatment

Table 2 shows representative SEM images of the obtained fiber mats without and with the 10 min-UV treatment. Diameters of the individual fiber segments were also reported in the table. All of the obtained fiber mats exhibited a common feature of smooth fiber segments with round cross-sections. Without the UV treatment, the diameters of the obtained fiber segments decreased significantly upon the initial addition of $AgNO_3$ into the base PAN solution. Further increase in the initial $AgNO_3$ concentration resulted in a slight and gradual decrease in the fiber diameters. The decrease in the diameters of the fiber segments should be a result of the increase in the charge density, in response to the observed increase in the electrical conductivity, of the spinning solutions. The increased charge density leads to greater electrical forces that are responsible for the elongation of the ejected jet during its transportation to the collecting device.[17,43]

The effect of the UV treatment on the morphology and size of the as-formed AgNPs within the electrospun fibers was investigated by TEM and the results are summarized in Table 3. Apparently, the as-formed AgNPs were spherical in shape with narrow size distribution. Without the UV treatment, the size of the as-formed AgNPs was less than 5 nm, regardless of the initial $AgNO_3$ concentration. The existence and the amount of the AgNPs within the fiber mats were further evaluated by EDX. For the fibers that had been prepared from the PAN solutions that contained 0.5, 1.5 and 2.5 wt.% of $AgNO_3$ and had been aged for 5 d, the detected amounts of the elemental Ag^0 were 0.067 ± 0.007, 0.117 ± 0.010 and 0.293 ± 0.003 wt.%, respectively. Evidently, the detected amount of the elemental Ag^0 increased

with an increase in the initial $AgNO_3$ concentration. Notwithstanding, these values were much lower than the content of the silver that should be present within the fibers. The large discrepancy from the theoretical values could be explained based on a number of reasons: 1) only partial amounts of Ag^+ ions were reduced into elemental Ag^0 and/or 2) only partial amounts of the elemental Ag^0 (i.e., AgNPs) were detected by the X-ray beam.

Further reduction of the residual Ag^+ ions could be achieved by UV irradiation. Upon the treatment of the fiber mat specimens with UV radiation, the photoreduction of Ag^+ ions could proceed according to the following mechanism:

$$AgNO_3 \longrightarrow Ag^0 + NO_2 + 1/2O_2. \quad (4)$$

According to the SEM images shown in Table 2, morphology of the irradiated fiber mat samples was essentially the same as that of the untreated ones. Similar results on the relationship between the diameters of the fiber segments and the initial $AgNO_3$ concentration could easily be recognized. However, the diameters of the irradiated fibers were consistently lower than those of the untreated ones. This could be a result of the effective removal of residual solvent and/or absorbed moisture during the irradiation process.

With the UV treatment, the as-formed AgNPs were also present as spherical entities (see Table 3). Compared with the untreated samples, a larger number of AgNPs were observed adjacent to and at the fiber surface after the UV treatment. For the fiber mat samples that had been treated for 1 min, no noticeable change in the size of the as-formed AgNPs was observed. Marked increase in the size of the as-formed AgNPs was observed for the samples that had been irradiated for 10 min and the size of these particles was an increasing function of the initial concentration of the as-loaded $AgNO_3$. The obtained results clearly suggested that UV treatment was responsible for further reduction of the residual Ag^+ ions within the fibers, but it occurred more effectively in areas of the fibers where the UV radiation was most accessible (i.e., adjacent to and at the fiber surface).

3.4.3 Dissolution and water retention behavior

The dissolution and ability to retain certain amount of water of a fibrous membrane are important properties determining the actual applicability of the

material. Despite the fact that PAN is a water-insoluble material, it is still necessary to investigate the behavior of the neat and the AgNPs-loaded PAN fiber mats upon their submersion in distilled water. The loss in the weight of the neat and the AgNPs-loaded PAN fiber mats prior to the UV irradiation in distilled water was low, with the average values ranging between 3.3 and 3.8%. On the other hand, the water retention of these fibrous materials was relatively high (i.e., ranging between 981 and 995%). No statistical difference among the various data groups was, however, observed. While the low weight loss should be attributable to the insolubility of the base material (i.e., PAN) in water, the relatively high water retention should be a result of the hydrophilicity of the base material and the ability of the fibrous membranes to retain a relatively large amount of water within the interfibrous spaces as a result of the capillary action. Though not shown, the morphology of these fiber mats after submersion in distilled water was unaffected.

3.4.4 Mechanical integrity

Mechanical integrity of a fibrous membrane is also an important property determining its actual applicability. The results for the neat and the AgNPs-loaded PAN fiber mats prior to the UV irradiation are reported in terms of the tensile strength and the elongation at break in Figure 2. Even though the tensile strength was found to increase slightly with the addition and increasing initial concentration of $AgNO_3$, these groups of data were not statistically different. A reverse trend was observed for the elongation at break that showed a slight decrease in the property values with the addition and increasing initial concentration of $AgNO_3$, but, again, no statistical difference was detected among these data groups.

3.4.5 Release characteristic of silver

The theoretical contents of silver, regardless of its form, within the fiber mats that had been prepared from the PAN solutions containing 0.5, 1.5 and 2.5 wt.% of $AgNO_3$ were about 3.1, 9.3 and 15.5 mg/g of the fiber mats, respectively. If these amounts of silver were all to be released into the dissolution medium (i.e., 50 mL of distilled water), the concentrations of silver in the corresponding medium would have been 62.0, 185.9 and 309.6 ppm/g of the fiber mats, respectively. By totally dissolving the AgNPs-loaded PAN fiber mats both before and after the UV treatment in HNO_3, the actual amounts of silver within the fiber mats were,

respectively, determined to be 2.9, 8.6-9.0 and 14.4-15.3 mg/g of the fiber mats on average (see Table 4). These values were later used as the basis for the calculation of the cumulative amounts of silver released from the fiber mat specimens into distilled water in the release assay.

With or without the UV treatment, relatively large amounts of silver were able to be released into water within the first day of immersion, as shown in Figure 3. Specifically, before the UV treatment, the cumulative amounts of the released silver for the fiber mats that had been prepared from the PAN solutions containing 0.5, 1.5 and 2.5 wt.% of $AgNO_3$ were about 0.5, 1.9 and 7.1 mg/g of the fiber mats (or 9.7, 38.7 and 141.7 ppm/g of the fiber mats), respectively. On the other hand, after the UV treatment, they were about 1.9, 3.0 and 8.9 mg/g of the fiber mats (or 38.0, 60.8 and 178.5 ppm/g of the fiber mats), respectively. These values increased gradually to about 0.6, 2.3 and 10.0 mg/g of the fiber mats (or 12.3, 46.3 and 201.5 ppm/g of the fiber mats) for the untreated AgNPs-loaded PAN fiber mats that had been immersed in distilled water for 7 d. On the other hand, they were about 2.9, 3.6 and 10.5 mg/g of the fiber mats (or 57.0, 72.8 and 211.7 ppm/g of the fiber mats) for the UV-treated counterparts. Evidently, the released amounts of silver from the fiber mats that had been irradiated with UV for 10 min were greater than those from the untreated ones. This is likely a result of the formation of a large number of AgNPs adjacent to and at the surface of the fibers (see Table 3).

3.4.6 Antibacterial activity

The antibacterial activity of the AgNPs-loaded PAN fiber mats that had been or had not been irradiated with UV for 1, 5 and 10 min was assessed against *S. aureus* and *E. coli*. The activities of the neat PAN fiber mats and the standard drugs against the tested microbes were used as controls. The lengths of the inhibition zones of the specimens (i.e., measuring from the edge of the fiber mat specimens to the edge of the inhibition zones) were analyzed and are reported in Figure 4.

As for the neat PAN fiber mats, no inhibition zones were observed against both types of bacteria, a result that is in line with the non-bactericidal property of the neat materials. On the other hand, inhibitory zones were obvious for all of the AgNPs-containing specimens. Apperently, the lengths of the inhibition

zones generally increased with increases in both the initial concentration of $AgNO_3$ in the PAN solution and the UV irradiation time interval and the antibacterial activity of the materials was more effective against *E. coli*. The increase in the antibacterial activity with an increase in the initial $AgNO_3$ concentration was due to the increased amounts of Ag^+ ions and the as-formed AgNPs within the obtained fibers, which, in turn, were responsible for the increased amounts of the as-released silver (see Figure 3). On the other hand, the increase in the antibacterial activity with an increase in the UV irradiation time interval should be a result of the additional photoreduction of Ag^+ ions into AgNPs that occurred in the layers of the fibers that were adjacent to and at their surface (see Table 3). The results also suggested that the photoreduction of Ag^+ ions into AgNPs should be driven by the diffusion of Ag^+ ions from the interior of the fibers toward the fiber surface, which could be the main reason for the enhancement in the actibacterial activity of the irradiated materials.

Lastly, the effectiveness of the as-released silver against *E. coli* was postulated to be a result of thinner peptidoglycan layer within their cell wall, as compared with that of *S. aureus* (7-8 nm versus 20-80 nm).[44,45] The thick peptidoglycan layer within the cell wall of Gram-positive bacteria like *S. aureus* contains teichoic and lipoteichoic acids which act as chelating agents and could take part in the neutralization of the Ag^+ ions.[46]

3.5 Conclusion

Polyacrylonitrile (PAN) in its compositing with silver nanoparticles (AgNPs) was successfully prepared in the form of fibrous membranes by electrospinning. The formation of AgNPs occurred in two steps: 1) the chemical reduction with DMF, which was also used as the solvent for the preparation of the spinning solutions (i.e., 10% w/v PAN solutions in DMF containing silver nitrate ($AgNO_3$) at 0.5, 1.5 and 2.5% by weight of PAN) and 2) subsequent reduction with UV irradiation. The presence of $AgNO_3$ in the PAN solutions resulted in a dramatic decrease in the diameters of the obtained fiber segments, while an increase in the initial $AgNO_3$ concentration in the solutions and the treatment of the obtained fibers

with UV irradiation resulted in a slight reduction of the fiber diameters. Without the UV treatment, the size of the as-formed AgNPs was independent of the initial $AgNO_3$ concentration in the solutions. With the UV treatment, the size of the as-formed AgNPs increased with both the UV treatment time and the initial $AgNO_3$ concentration in the solutions. The cumulative amounts of the as-released silver, either in the form of free ions or AgNPs, in distilled water at room temperature (i.e., 25 ± 1 °C) increased with increases in the submersion time, the initial $AgNO_3$ concentration in the solutions and the UV irradiation time interval. Lastly, the antibacterial activity of the AgNPs-loaded PAN fiber mats against two bacterial strains, i.e., *S. aureus* and *E. coli*, increased with increases in the initial $AgNO_3$ concentration in the solutions and the UV irradiation time interval.

3.6 Acknowledgments

The authors acknowledged partial support from (a) the National Nanotechnology Center (grant number: BR0108), (b) the Center for Petroleum, Petrochemicals and Advanced Materials (C-PPAM), and (c) the Petroleum and Petrochemical College (PPC), Chulalongkorn University. PR acknowledged a doctoral scholarship received from the Thailand Graduate Institute of Science and Technology (TGIST) (TG-55-09-49-067D).

3.7 References

1. Iijima S, Ichihashi T. Structural instability of ultrafine particles of metals. Physical Review Letters 1986;56:616-619.
2. Ajayan PM, Marks LD. Quasimelting and Phases of Small Particles. Physical Review Letters 1988;60:585-587.
3. Wright JB, Hansen DL, Burrell RE. The comparative efficacy of two antimicrobial barrier dressings: in vivo examination of two controlled release silver dressings. Wounds 1998;10:179-188.
4. Somorjai GA. On the Move. Nature 2004;430:730.

5. Tian J, Wong KKY, Ho CM, Lok CN, Yu WY, Che CM, Chiu JF, Tam PKH. Topical Delivery of Silver Nanoparticles Promotes Wound Healing. ChemMedChem 2006;2:129-136.
6. Kong H, Jang J. Antibacterial Properties of Novel Poly(methyl methacrylate) Nanofiber Containing Silver Nanoparticles. Langmuir 2008;24:2051-2056.
7. Lok CN, Ho CM, Chen R, He QY, Yu WY, Sun H, Tam PKH, Chiu JF, Che CM. Proteomic analysis of the mode of antibacterial action of silver nanoparticles. Journal of Proteome Research 2006;5:916-924.
8. Solomon SD, Bahadory M, Jeyarajasingam AV, Rutkowsky SA, Boritz C. Synthesis of Silver Nanoparticles. Journal of Chemical Education 2007;84:322-325.
9. Luong ND, Lee Y, Nam JD. Highly-loaded silver nanoparticles in ultrafine cellulose acetate nanofibrillar aerogel. European Polymer Journal 2008;44:3116-3121.
10. Maneerung T, Tokura S, Rujiravanit R. Impregnation of silver nanoparticles into bacterial cellulose for antimicrobial wound dressing. Carbohydrate Polymers 2008;72:43-51.
11. Zhang W, Qiao X, Chen J, Wang H. Preparation of Silver Nanoparticles in Water-in-oil AOT Reverse Micelles. Journal of Colloid and Interface Science 2006;302:370-373.
12. Maria LCS, Santos ALC, Oliveira PC, Barud HS, Messaddeq Y, Ribeiro SJL. Synthesis and characterization of silver nanoparticles impregnated into bacterial cellulose. Materials Letters 2009;63:797-799.
13. Dong F, Li Z, Huang H, Yang F, Zheng W, Wang C. Fabrication of semiconductor nanostructures on the outer surfaces of polyacrylonitrile nanofibers by in-situ electrospinning. Materials Letters 2007;61:2556-2559.
14. Song X, Jun L, Li Z, Li S, Wang C. Synthesis of polyacrylonitrile/Ag core–shell nanowire by an improved electroless plating method. Materials Letters 2008;62:2681-2684.
15. Wang Y, Yang Q, Shan G, Wang C, Du J, Wang S, Li Y, Chen X, Jing X, Wei Y. Preparation of silver nanoparticles dispersed in polyacrylonitrile nanofiber film spun by electrospinning. Materials Letters 2005;59:3046-3049.

16. Yang QB, Li DM, Hong YL, Li ZY, Wang C, Qui SL, Wei Y. Preparation and characterization of a PAN nanofibre containing Ag nanoparticles via electrospinning. Synthetic Metals 2003;137:973-974.
17. Lee HK, Jeong EH, Baek CK, Youk JH. One-step preparation of ultrafine poly(acrylonitrile) fibers containing silver nanoparticles. Materials Letters 2005;59:2977-2980.
18. Zhang Z, Han M. One-step preparation of size-selected and well-dispersed silver nanocrystals in polyacrylonitrile by simultaneous reduction and polymerization. Journal of Materials Chemistry 2003;13:641-643.
19. Son WK, Youk JH, Lee TS, Park WH. Antimicrobial cellulose acetate nanofibers containing silver nanoparticles. Carbohydrate Polymers 2006;65:430-434.
20. Hong KH, Park JL, Sul IN, Youk JH, Kang TJ. Preparation of antimicrobial poly(vinyl alcohol) nanofibers containing silver nanoparticles. Journal of Polymer Science B: Polymer Physics 2006;44:2468-2474.
21. Yoksan R, Chirachanchai S. Silver nanoparticles dispersing in chitosan solution: Preparation by γ-ray irradiation and their antimicrobial activities. Materials Chemistry and Physics 2009;115:296-302.
22. Torreggiani A, Jurasekova Z, D'Angelantonio M, Tamba M, Garcia-Ramos JV, Sanchez-Cortes S. Fabrication of Ag nanoparticles by γ-irradiation: Application to surface-enhanced Raman spectroscopy of fungicides. Colloids and Surfaces A: Physicochemical and Engineering Aspects 2009;339:60-67.
23. Rather S, Naik M, Hwang SW, Kim AR, K Nahm KS. Room temperature hydrogen uptake of carbon nanotubes promoted by silver metal catalyst. Journal of Alloys and Compounds 2009;475:L17-L21.
24. Gorczynski RM, Macrae S, Kennedy M. Conditioned immune response associated with allogeneic skin grafts in mice. Journal of Immunology 1982;129:704-709.
25. Jin WJ, Lee HK, Jeong EH, Park WH, Youk JH. Preparation of polymer nanofibers containing silver nanoparticles by using poly(N-vinylpyrrolidone). Macromolecular Rapid Communications 2005;26:1903-1907.

26. Reneker DH, Yarin AL. Electrospinning jets and polymer nanofibers. Polymer 2008;49:2387-2425.
27. Beachley V, Wen X. Effect of electrospinning parameters on the nanofiber diameter and length. Materials Science and Engineering C 2009;29:663-668.
28. Han T, Yarin AX, Reneker DH. Viscoelastic electrospun jets: Initial stresses and elongational rheometry. Polymer 2008;49:1651-1658.
29. Dersch R, Graeser M, Greiner A, Wendorff JH. Electrospinning of nanofibres: Towards new techniques, functions, and applications. Australian Journal of Chemistry 2007;60:719-728.
30. Liang D, Hsiao BS, Chu B. Functional electrospun nanofibrous scaffolds for biomedical applications. Advanced Drug Delivery Reviews 2007;59:1392–1412.
31. Schreuder-Gibson HL, Gibson P, Tsai P, Gupta P, Wilkes G. Cooperative charging effects of fibers from electrospinning of electrically dissimilar polymers. International Nonwovens Journal 2004;13:39–45.
32. Chen C, Wang L, Huang Y. Ultrafine electrospun fibers based on stearyl stearate/polyethylene terephthalate composite as form stable phase change materials. Chemical Engineering Journal 2009;150:269-274.
33. Gibson P, Schreuder-Gibson H, Rivin D. Transport properties of porous membranes based on electrospun nanofibers. Colloids and Surfaces. A: Physicochemical and Engineering Aspects 2001;187-188:469–481.
34. Nam-Wun O, Jegal J, Kew-Ho L. Preparation and characterization of nanofiltration composite membranes using polyacrylonitrile (PAN). I. Preparation and modification of PAN supports. Journal of Applied Polymer Science 2001;80:1854-1862.
35. Wang J, Yue Z, Scott J, Ince J. Economy preparation of nanofiltration membranes from polyacrylonitrile ultrafiltration membranes. Journal of Membrane Science 2006;286:333-341.
36. Baumgarten PK, Electrostatic spinning of acrylic microfibers. Journal of Colloid and Interfacial Science 1971;36:71-79.
37. Sutasinpromprae J, Jitjaicham S, Nithitanakul M, Meechaisue C, Supaphol P. Preparation and characterization of ultrafine electrospun polyacrylonitrile

fibers and their subsequent pyrolysis to carbon fibers. Polymer International 2006;55:825-833.

38. Lee HK, Jeong EH, Baek CK, and Youk, JH. One-step preparation of ultrafine poly(acrylonitrile) fibers containing silver nanoparticles. Materials Letters 2005;59:2977-2980.
39. Xu X, Yang Q, Wang Y, Yu H, Chen X, Jing X. Biodegradable electrospun poly(L-lactide) fibers containing antibacterial silver nanoparticles. European Polymer Journal 2006;42:2081-2087.
40. Jeon HJ, Kim JS, Kim TG; Kim JH, Yu WR, Youk JH. Preparation of poly(e-caprolactone)-based polyurethane nanofibers containing silver nanoparticles. Applied Surface Science 2008;254:5886-5890.
41. Rujitanaroj P, Pimpha N, Supaphol P. Wound-dressing materials with antibacterial activity from electrospun gelatin fiber mats containing silver nanoparticles. Polymer 2008;49:4723-4732.
42. Yakutik IM, Shevchenko GP. Self-organization of silver nanoparticles forming on chemical reduction to give monodisperse spheres. Surface Science 2004;566-568:414-418.
43. Son WK, Youk JH, Lee TS, Park WH. The effects of solution properties and polyelectrolyte on electrospinning of ultrafine poly(ethylene oxide) fibers. Polymer 2004;45:2959-2966.
44. Feng QL, Wu J, Chen GQ, Cui FZ, Kim TN, Kim JO. A mechanistic study of the antibacterial effect of silver ions on *Escherichia coli* and *Staphylococcus aureus*. Journal of Biomedical Materials Research 2000;52:662-668.
45. Anomymous. Peptidoglycan. http://en.wikipedia.org/wiki/Peptidoglycan, accessed June 4th, 2009.
46. Anomymous. Gram-positive bacteria. http://en.wikipedia.org/wiki/Gram-positive_bacteria, accessed June 4th, 2009.

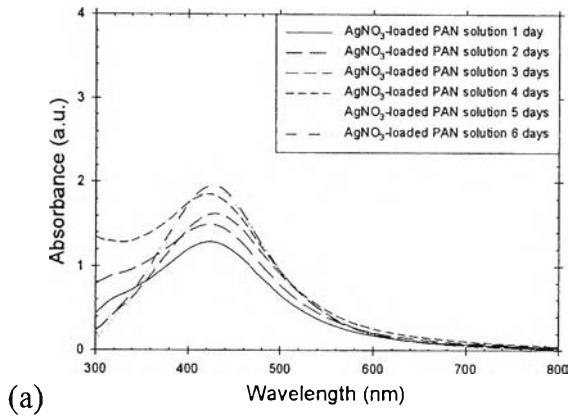

(a)

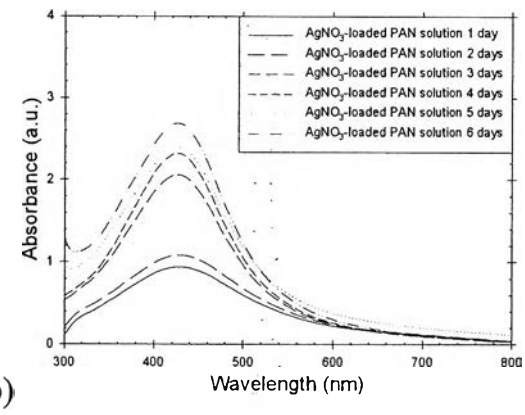

(b)

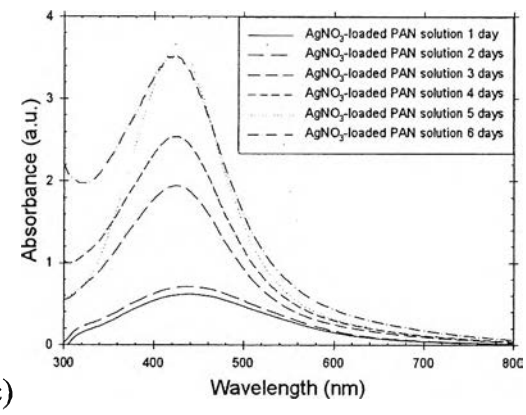

(c)

Figure 1. Changes in UV-visible absorption spectra of 10% w/v PAN solution in DMF containing various amounts of $AgNO_3$ of (a) 0.5, (b) 1.5 and (c) 2.5% by weight of PAN after having been aged for various time intervals (n = 3).

Table 1. Shear viscosity and electrical conductivity of the base PAN solution and the $AgNO_3$-containing PAN solutions that had been aged for 5 d ($n = 3$).

Type of solution	Viscosity (mP.s)	Conductivity ($\mu S \cdot cm^{-1}$)
10% w/v PAN solution in DMF	337.2 ± 0.2	58.2 ± 0.31
10% w/v PAN solution in DMF containing $AgNO_3$ at 0.5% by weight of PAN	342.4 ± 0.3	151.3 ± 0.84
10% w/v PAN solution in DMF containing $AgNO_3$ at 1.5% by weight of PAN	352.1 ± 0.4	248.7 ± 1.92
10% w/v PAN solution in DMF containing $AgNO_3$ at 2.5% by weight of PAN	362.8 ± 0.3	319.1 ± 0.12

Table 2. Representative SEM images illustrating morphology and diameters of electrospun fibers from 10% w/v PAN solution in DMF and the 5 d-aged solutions that contained $AgNO_3$ in the amounts of 0.5-2.5% by weight of PAN without and with 10 min of UV irradiation.

Type of material	Fibers from 10% w/v PAN solution in DMF	Fibers from 10% w/v PAN solution in DMF containing $AgNO_3$ at 0.5% by weight of PAN	Fibers from 10% w/v PAN solution in DMF containing $AgNO_3$ at 1.5% by weight of PAN	Electrospun fibers from 10% w/v PAN solution in DMF containing $AgNO_3$ at 2.5% by weight of PAN
No UV treatment	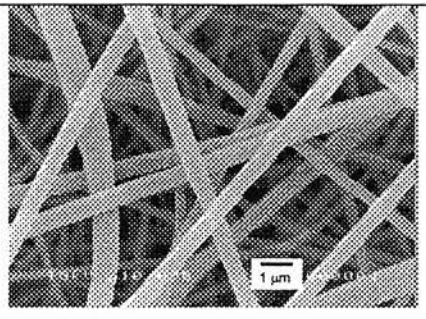	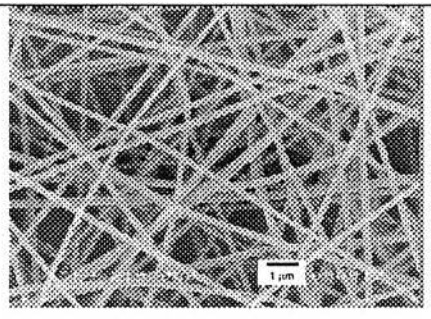	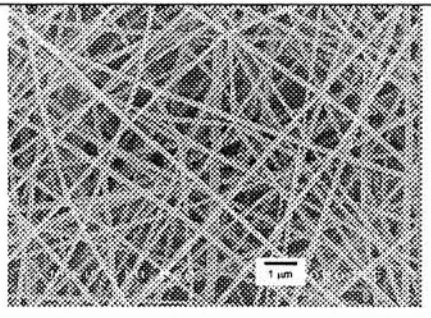	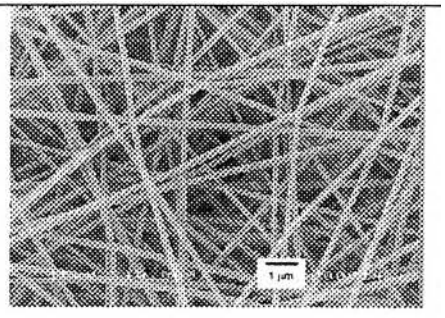
	649 ± 53 nm	236 ± 29 nm	213 ± 38 nm	194 ± 30 nm
With UV treatment for 10 min	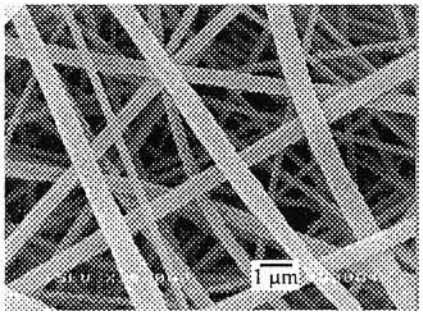	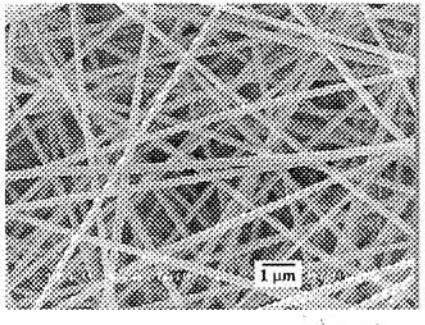	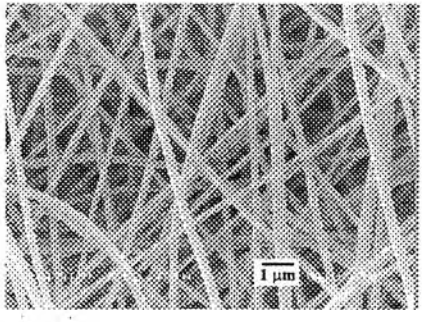	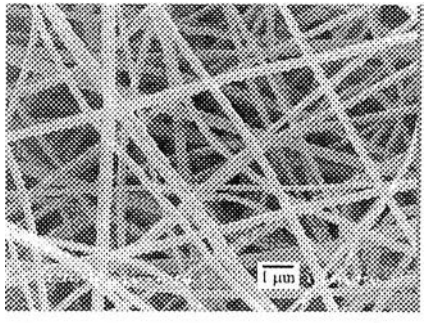
	629 ± 48 nm	205 ± 44 nm	197 ± 21 nm	185 ± 34 nm

Table 3. Representative TEM images illustrating distribution, morphology and diameters of AgNPs that were formed within electrospun fibers from 5 d-aged 10% w/v PAN solutions in DMF that contained $AgNO_3$ in the amounts of 0.5-2.5% by weight of PAN without and with 1 or 10 min of UV irradiation.

Type of material	Fibers from 10% w/v PAN solution in DMF containing $AgNO_3$ at 0.5% by weight of PAN	Fibers from 10% w/v PAN solution in DMF containing $AgNO_3$ at 1.5% by weight of PAN	Fibers from 10% w/v PAN solution in DMF containing $AgNO_3$ at 2.5% by weight of PAN
No UV treatment	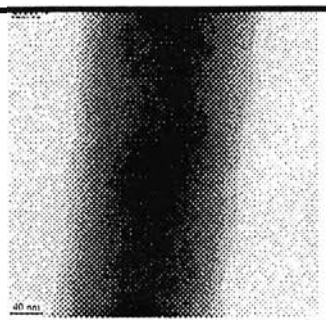 < 5 nm	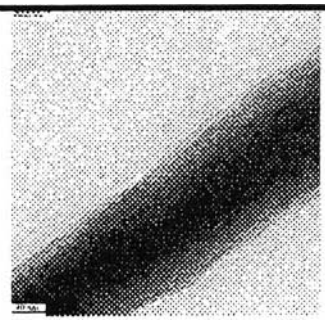 < 5 nm	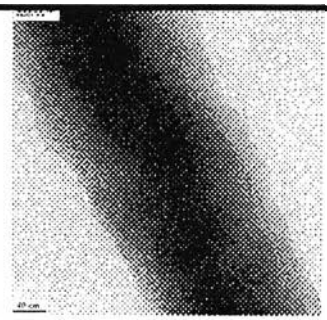 < 5 nm
With UV treatment for 1 min	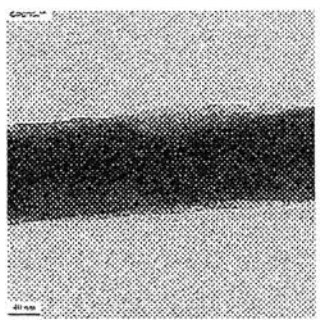 4.4 ± 0.5 nm	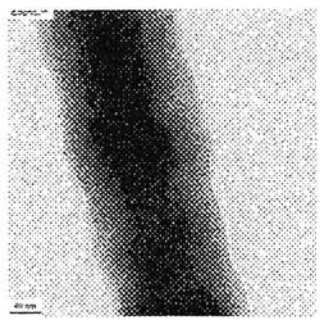 4.0 ± 0.4 nm	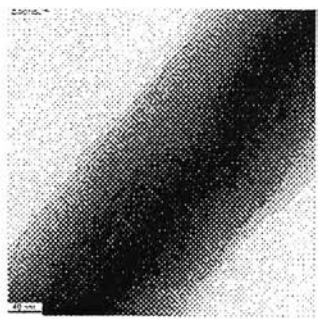 5.2 ± 0.3 nm

Table 3. Representative TEM images illustrating distribution, morphology and diameters of AgNPs that were formed within electrospun fibers from 5 d-aged 10% w/v PAN solutions in DMF that contained $AgNO_3$ in the amounts of 0.5-2.5% by weight of PAN without and with 1 or 10 min of UV irradiation (continued).

Type of material	Fibers from 10% w/v PAN solution in DMF containing $AgNO_3$ at 0.5% by weight of PAN	Fibers from 10% w/v PAN solution in DMF containing $AgNO_3$ at 1.5% by weight of PAN	Fibers from 10% w/v PAN solution in DMF containing $AgNO_3$ at 2.5% by weight of PAN
With UV treatment for 10 min	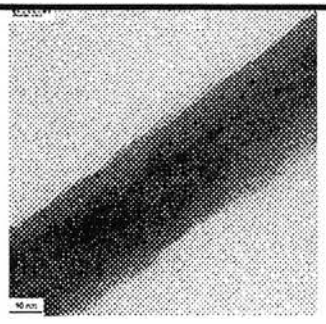	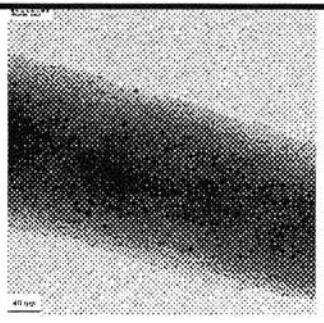	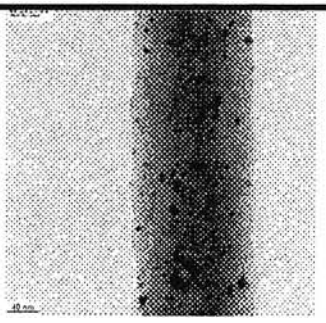
	5.3 ± 0.8 nm	6.2 ± 0.7 nm	7.8 ± 0.2 nm

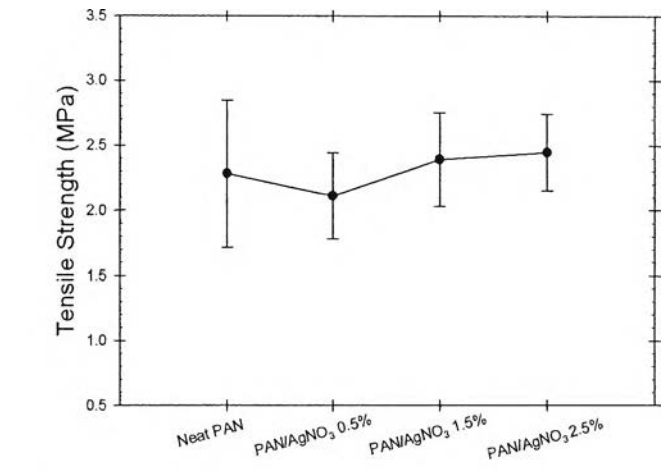

(a)

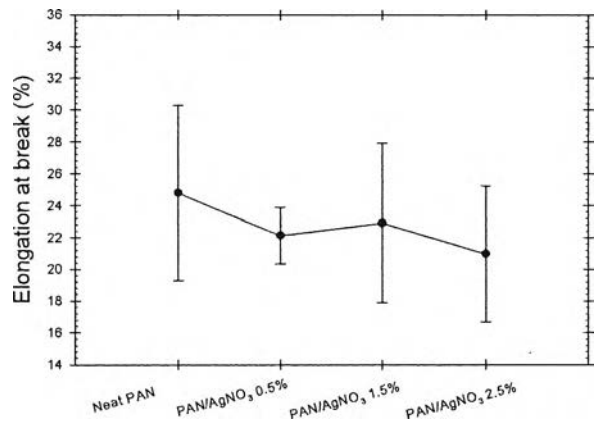

(b)

Figure 2. Mechanical integrity in terms of (a) tensile strength and (b) elongation at break of electrospun fiber mats from 10% w/v PAN solution in DMF and the 5 d-aged solutions that contained $AgNO_3$ in the amounts of 0.5-2.5% by weight of PAN without UV irradiation (n = 10).

Table 4. Actual amounts of silver in electrospun fiber mats from 5 d-aged 10% w/v PAN solutions in DMF that contained $AgNO_3$ in the amounts of 0.5-2.5% by weight of PAN both before and after 10 min of UV treatment ($n = 3$).

Type of material	Actual amount of silver before UV irradiation	Actual amount of silver after UV irradiation
Fiber mats from 10% w/v PAN solution in DMF containing $AgNO_3$ at 0.5% by weight of PAN	2.94 ± 0.04 mg/g[a] or 58.8 ± 0.8 ppm/g[a] or 94.9 ± 1.3%[b]	2.93 ± 0.04 mg/g[a] or 58.6 ± 0.8 ppm/g[a] or 94.6 ± 1.3%[b]
Fiber mats from 10% w/v PAN solution in DMF containing $AgNO_3$ at 1.5% by weight of PAN	8.60 ± 0.08 mg/g[a] or 172.0 ± 1.6 ppm/g[a] or 92.5 ± 0.9%[b]	9.00 ± 0.23 mg/g[a] or 180.0 ± 4.6 ppm/g[a] or 96.8 ± 2.5%[b]
Fiber mats from 10% w/v PAN solution in DMF containing $AgNO_3$ at 2.5% by weight of PAN	14.44 ± 0.28 mg/g[a] or 288.8 ± 5.6 ppm/g[a] or 93.2 ± 1.8%[b]	15.30 ± 0.42 mg/g[a] or 306.0 ± 8.4 ppm/g[a] or 98.8 ± 2.7%[b]

[a] based on the weight of the fiber mat samples

[b] based on the weight of silver initially loaded in the solution

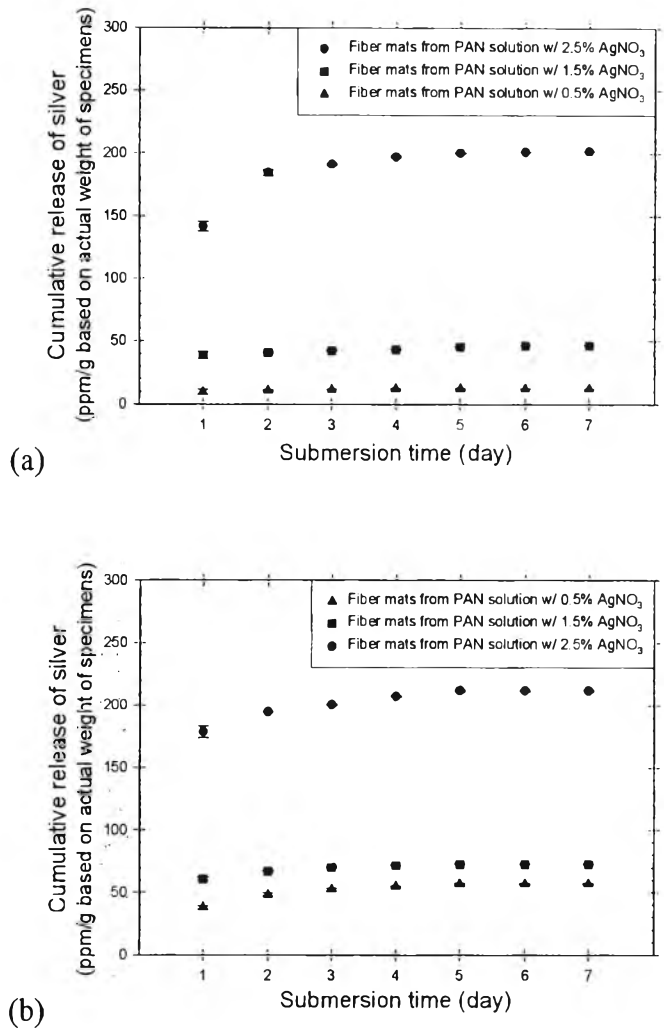

Figure 3. Cumulative release profiles of silver from electrospun fiber mats from 5 d-aged 10% w/v PAN solutions in DMF that contained $AgNO_3$ in the amounts of 0.5-2.5% by weight of PAN both (a) before and (b) after 10 min of UV treatment upon total submersion in distilled water at room temperature (i.e., 25 ± 1 °C) (n = 3).

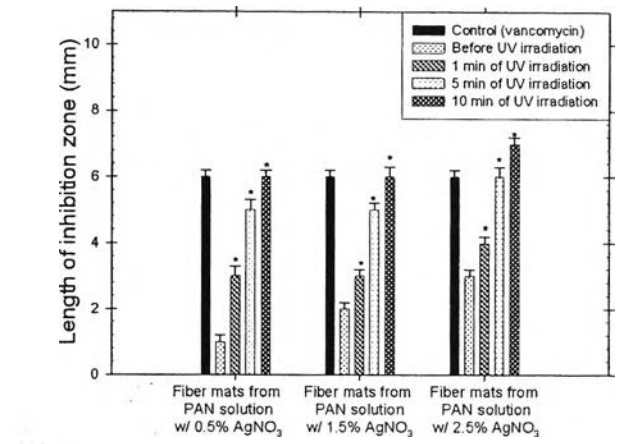

(a)

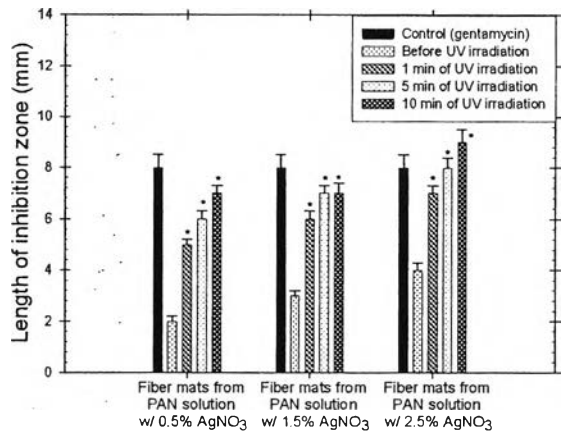

(b)

Figure 4. Lengths of inhibition zones illustrating the antibacterial activity of electrospun fiber mats from 5 d-aged 10% w/v PAN solutions in DMF that contained $AgNO_3$ in the amounts of 0.5-2.5% by weight of PAN both before and after 1, 5 and 10 min of UV treatment against (a) Gram-positive *Staphylococcus aureus* and (b) Gram-negative *Escherichia coli* (n = 3). The original diameters of the fiber mat specimens were 15 mm and those of gentamicin and vancomycin disks were 6 mm. (*) $p < 0.05$, compared with the fiber mat specimens before the UV treatment.